SENSITIVITY ANALYSIS OF CFD FOR LIQUID METAL FLOW IN FUEL BUNDLE SIMULATORS IN THE IAEA COORDINATED RESEARCH PROJECT CRP-I31038

Abdalla Batta, Andreas G. Class
Karlsruher Institut für Technologie (KIT)
Hermann-von-Helmholtz-Platz 1,
76344 Eggenstein-Leopoldshafen Germany
abdalla.batta@kit.edu, class.andreas@kit.edu

Abstract

Innovating fast reactor design towards implementation heavily relies on computational studies accompanying generic experimental studies. Among the EU liquid metal cooled fast reactor concepts MYRRHA uses a wire-wrapped fuel bundle. The Coordinated Research Project (CRP) Benchmark of Transition from Forced to Natural Circulation Experiment with Heavy Liquid Metal Loop (NACIE)-CRP-I31038', is used for the validation of predictive capabilities of CFD and system codes at prototypic conditions. The Coordinated Research Project (CRP) Benchmark of Transition from Forced to Natural Circulation Experiment with Heavy Liquid Metal Loop (NACIE)-CRP-I31038', is used for the validation of predictive capabilities of our modelling approach.

KIT with its decades of experience in liquid metal flow simulation contributed to the CFD work package. Participants from many countries demonstrated that predictions nicely capture the flow structure and heat transfer within the NACIE-loop. Yet in the blind case of the benchmark, an average error of the order of approximately 10-60% between experiment and CFD simulation is reported for cases with strongly asymmetric heating. The KIT results are among the best candidates and use numerical methods that could be applied in industrial simulations.

A detailed sensitivity analysis of the KIT simulations and experimental data is undertaken to explain the origin of these uncertainties. The sensitivity of measurement locations will be highlighted, as it can explain a part of the possible deviations. It can be shown that in case of asymmetric heating large gradients of temperature are observed and that small displacement of measurement positions results in a better agreement between experiments and simulation. On top of this spatial uncertainty the operational parameters and material properties also show similar uncertainty as our numerical prediction. In the design of a future liquid metal fast reactors CFD will provide reliable results. We recommend that multiple independent studies are performed and sensitivity data is produced.

1 INTRODUCTION

The qualification of CFD codes through validation enhances confidence in the applied models for the design of advanced liquid metal reactor features. The benchmark on the transition from forced to natural circulation, conducted using the heavy liquid metal loop (CRP-I31038) organized by the IAEA, is an important reference for validating numerical design tools, including system codes and CFD models, under both transient and steady flow conditions. The experimental data for this benchmark are taken from the NAtural CIrculation Experiment–UPgraded facility (NACIE-UP). The experiment was carried out by the ENEA Brasimone Research Centre (Italy). Detailed information on the benchmark objectives and specifications is provided in [1,2]. KIT participates in the CFD work package of the Coordinated Research Project (CRP). The benchmark provides data for natural and forced convection under three heating modes: fully symmetrical heating, symmetrical central heating, and asymmetrical heating. The tested bundle consists of 19 pins. Fig. 1 shows the CAD drawing of the test section along with the origin of the coordinate system used. The flow direction, indicated by an arrow in Fig. 1, is opposite to gravity; i.e., the flow is upward. Fig. 2 shows a cross-section of the bundle and illustrates the three heating configurations. The activated heaters in each test are highlighted in red.

Within the benchmark, 12 participants share their standalone CFD data for validation enabling the investigation of numerous expert selections of parameters for the simulation. Material properties and inlet condition are fixed in this benchmark. The geometrical and numerical parameters are decided by participants for their own simulation. See [3] for details. KIT benchmark results for all cases were published in [4-6]. The CFD model selection was optimized employing the data of the forced convection case ADP10 in [4]. KIT results show good agreement compared to experimental results. The comparison of benchmark participants in [3] for all cases considering the wire wrap shows that all CFD results generally capture the trend of temperature distribution quite well for uniform symmetric heating. All temperature predictions are seen to be within 8°C compared to the

experimental measurements at any TC location, which is about 11% of the total temperature rise in the bundle. This observation agrees well with former study of [7] where a review of CFD RANS methodologies for wire-wrapped bundles reported that flow and heat transfer can be predicted with an accuracy estimate of 12.5%.

Table 1 shows blind-phase KIT results compared to maximum and minimum errors found by other benchmark participants. Participant's data who ignore the wire wrap, i.e. consider bare rods, shows very high error; accordingly, they are excluded in the comparison in this study. The local error value is defined in the benchmark as avg. Error (%) = 100*$|T_{CFD}-T_{exp}|/(T_{exp}-T_{101})$, where $TCFD$ is the local temperature prediction by CFD, T_{exp} is the local temperature measurement by experiments, and $T101$ is the temperature at the inlet of the bundle upstream the inlet shown in Fig. 1. The maximum absolute temperature difference is defined by $|T_{CFD}-T_{exp}|$. It is presented in Table 1 as max. deviation (°C). The comparison in Table 1 indicates that our results are close to the best ranked one. We observe that temperatures measured by thermocouples (TCs) mounted on pins which are not actively heated or at locations away from the activated heaters rise the average error. TCs laying in actively heated regions - thus more relevant for safety considerations - show an error range that is comparable to the error observed in the symmetrically heated cases.

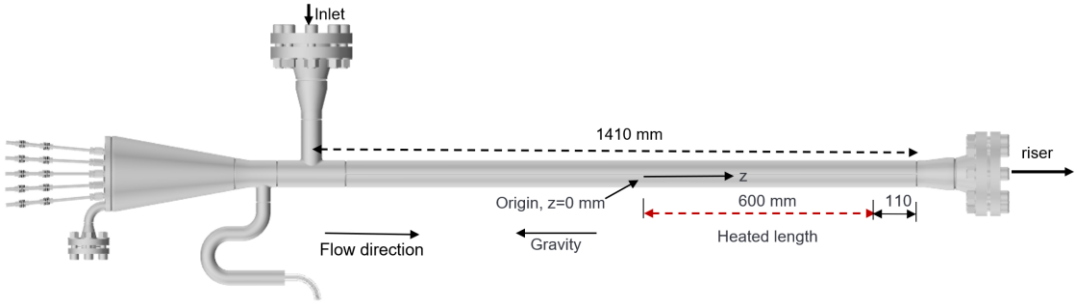

FIG. 1. CAD drawing of the test section and origin of the used coordinate system [4].

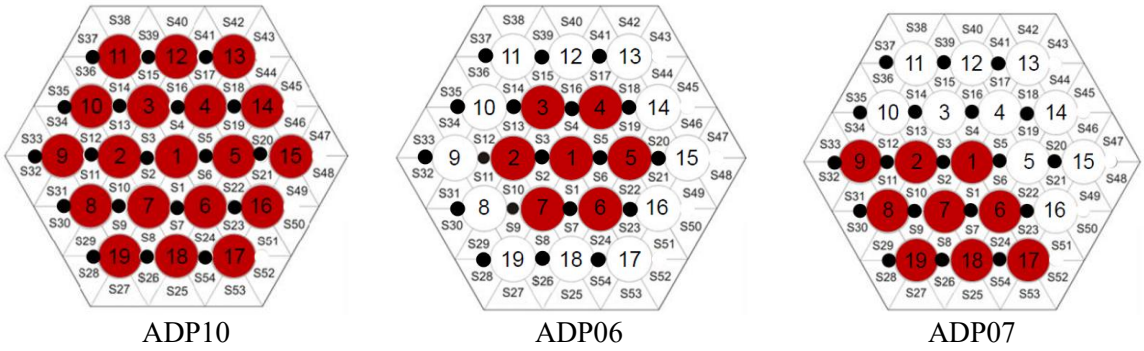

FIG. 2. Bundle cross section; test cases ADP10, ADP06 and ADP07; active pins (in red) [4].

TABLE 1. KIT RESULTS IN FORCED AND NATURAL CONVECTION ASYMMETRICALLY HEATED CASES ADP07 COMPARED TO BENCHMARK MAXIMUM AND MINIMUM.

	Avg. Error (%)		Max. Deviation (°C)		Overall rank
	Forced	Natural	Forced	Natural	Natural
Minimum	27.9	11.6	21.9	27.5	
KIT	36.5	13.9	36.8	28.7	5
Maximum	50.4	20.4	45.4	51.6	

The evaluation of the benchmark shows that, among reasons for reduced accuracy in the asymmetrically heated case, is the modelling of fluid mixing between the individual bundle subchannels. This may lead to large uncertainty in the predicted fields, when adjacent subchannels exhibit high temperature differences. In this case, a small under- or over-estimation in the mixing could result in higher errors compared to the symmetrically heated cases, where the temperature differences between neighbouring channels are expected to be lower. The best rank among the participants considering the symmetrically heated cases (open phase benchmark) was given to the results of Dollezhal Research and Development Institute of Power Engineering, Russia (NIKIET). They adapted

the turbulent Prandtl number Pr_t based on an independent DNS data analysis [8]. For this purpose, they performed a supplementary DNS simulation of a wire-wrapped bundle, to analyse the turbulent mixing in the bundle. A RANS-based parametric optimization was reported where the coefficients of the k-ω SST model were modified to obtain better mixing prediction in comparison to the DNS data. The modification was reported to be limited to changing the coefficient $a1$ from 0.31 to 0.26. NIKIET makes use of this modified k-ω SST model for all blind simulations [3]. However, the improved model did not meet the expectations for asymmetrically heated cases. We assume that new coefficients for the simulation of a reliable mixing in the bundle flow are required. Another effective parameter which is not considered by the benchmark participants is the sensitivity related to the exact measurement locations and possible displacement due to geometrical deformation. We speculate that this could contribute to the uncertainty of results.

To gain understanding of possible reasons behind the obtained high errors, the case of forced convection applying asymmetrical heating (ADP07ss1) is considered for the present detailed analysis. In addition, a sensitivity study to displacement, deformation or inaccurate measurement position is considered. Here a displacement relative to the original TC axial positions of ± 1 mm and ± 5° of azimuthal position around the rods is assumed. For our position displacement study, TCs on Pin3 are considered.

2 BENCHMARK DATA

Details of the benchmark can be found in [1,2]. Here, a short description of the data and essential specifications are presented. The tested fuel pin simulator (FPS) has 19 wire-wrapped pins. Fig. 1 illustrates the test section and specifies the origin of the used coordinate system. The heated section of the bundle is downstream of a preconditioner section and starts at z=0. The flow in the heated section is directed upward. Fig. 2 shows a cross section through the bundle and illustrates three heating configurations. For each heating configuration, experimental data for forced and natural convection are made available in form of temperature values at TCs located in the experiment. Temperatures are measured at defined positions in the subchannels and on the surfaces of the fuel pin simulator at three cross sections A, B and C as indicated in Fig. 3a. Additionally, the axial temperature variation along pin3 is measured by 13 thermocouples (numbered 55 to 67). Fig. 3b provides the positions and numbering of the TCs.

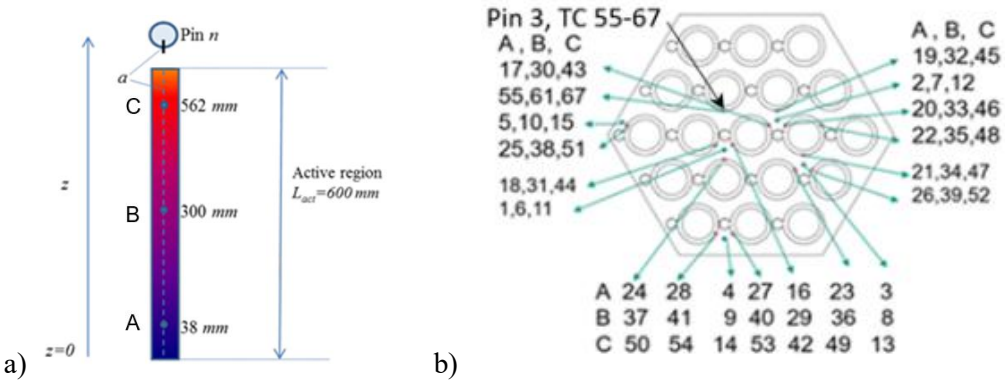

FIG. 3. (a) Location of planes for TC measurements in the test section (A at z= 38mm, B at z=300mm, and C at z=562mm) (b) location and numbering of thermocouples in measurements planes [4].

In Fig. 3b the green dots denote thermocouples positioned in the bulk fluid in 5 subchannels while red dots denote thermocouples measuring wall temperature on selected pin surfaces. Heating of pins is individually controlled enabling several heating configurations with a maximum power of 250 kW in total. All pins have identical maximum heating power. The active heated length of each pin is 600 mm. The bundle is characterised by the pin diameter of 6.55 mm; the triangular pitch of the FPS is 8.4 mm and the streamwise pitch is 262 mm. The resulting hydraulic diameter in the heated section is 3.84 mm.

Table 2 presents firstly the integral parameters for case ADP10ss1 (used for model selection in [4]) and secondly the studied case in this study ADP07ss1. Also see [6] for more details. Both cases are forced convection cases. The effective heating (Q_{eff}) in the heated and the preheating (Q_{pre}) in the preconditioning section are simulated. The Q_{tfm} is the power supplied to a thermal flow meter installed upstream of the test section which is

excluded in the simulation.

TABLE 2. INTEGRAL PARAMETERS OF CASE ADP10SS1 AND ADP07SS1.

	ADP10ss1 [1, rev1]			ADP07ss1 [1, rev5]		
Parameter	**Data**	**σ**	**σ[%]**	**Data**	**σ**	**σ[%]**
$\dot{m}_{gas}[Nl/min]$	10	0.5	5	10	0.5	5
$\dot{m}_{LBE}[kg/s]$	2.56	0.28	11	3.07	0.18	5.8
TP_{101}[°C]	225.4	1.5		237.16	1.5	
ΔT_{pre}[°C]	5,9	0.7	0.9	6.4	1.93	30.16
Q_{nom} [w]	30000	50	0.2	37996	45	0.12
Q_{eff} [w]	27000	1053	3.9	33935	1970	5.8
Q_{pre} [w]	2236	403	18	2873	847	29.5
Q_{tfm} [w]	1915	3	0.2	1960	3	0.13

3 NUMERICAL MODEL

The model used in the analysis of the blind case ADP07ss1 which is considered in this study was decided in the force convection steady-state open-phase case ADP10ss1, see [4] for more details. The model selection was based on previous experience gained at KIT for liquid metal bundle flows, see [9-12]. Table 2 presents the integral parameters of case ADP10ss1 and case ADP07ss1. In [4] two different approaches for the simulation of heaters were tried. The first approach considers the cladding of the fuel pin simulator (FPS) to represent the heater as shown in Fig. 4a. In this case the generated heat is simulated by a constant heat flux at the inner surface of the cladding. In the second approach all layers of the FPS are simulated as shown in Fig. 4a right.

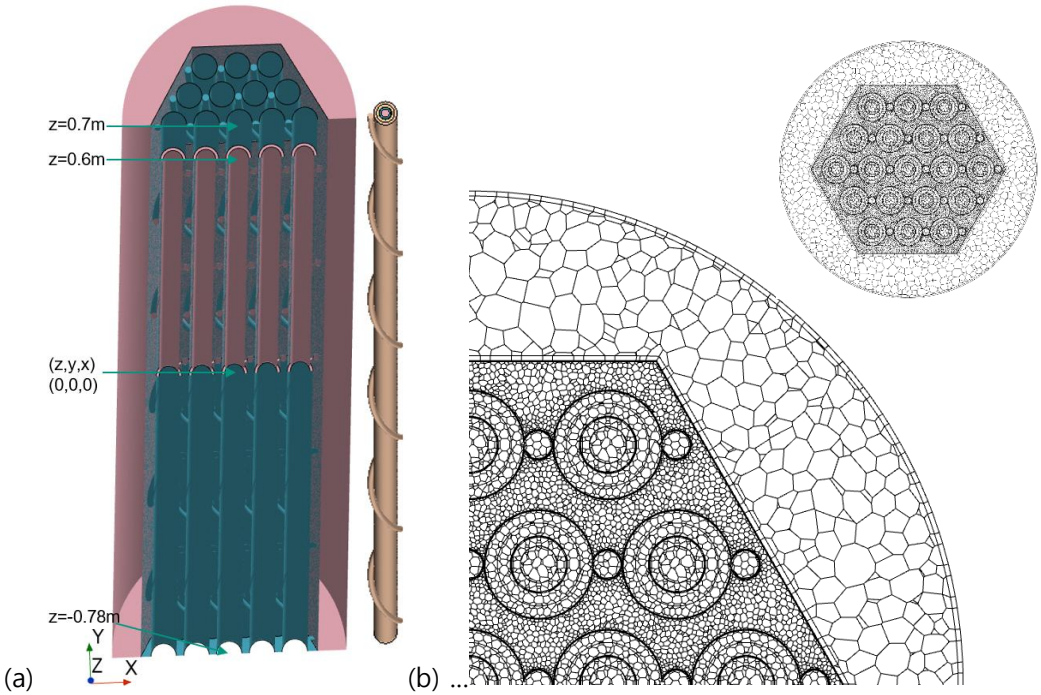

FIG. 4. a) Computational domain with short, simplified heater (left) and detailed simulated long heater (right). b) Cross section of meshes used in simulation.[4]

When studying the short heater, mesh I which has 49 M (Million) fluid cells and 13 M solid cells representing cladding and wrapper is used. In the second trail considering fully resolved heaters a more refined mesh II is used, comprising 96 M fluid cells and 29 M solid cells for the heater and wrapper. Fig. 4b shows a cross

section of the mesh II used in all simulations. In both trails the $T_{IN,\,FPS}$ was selected according to specification, so that in the first trail a constant inlet temperature was used. In the second trail the preheating was considered resulting in an average inlet temperature equal to that used in the first trail. The Star CCM+ CFD commercial code is used. For the simulation of prescribed testes, the SST turbulence model with "all y^+ wall treatment" is applied. In all calculations, buoyancy is considered. Isothermal conditions at outer surfaces are used. The inlet is selected uniform thus assuming that the flow will develop rapidly, so that fully developed conditions are reached before the heated region. This was agreed in the benchmark by all participants.

A second order advection scheme for velocity and temperature was used for all benchmark cases submitted by KIT. Later we found out that the first-order temperature advection scheme gives better convergence and more accurate results than the second order scheme. Accordingly, the first order advection scheme is used for the present study of ADP07ss1. A consistent agreement compared to experimental results is obtained for both the short and long heaters with mesh I and II. Yet, a slightly better agreement is obtained when fully resolved heaters and the finer mesh II are used. Therefore, they were used for the simulation of all benchmark cases.

The OECD handbook data [13] for the physical properties of LBE are used. The fuel pin simulators are fabricated from of several layers. For the outer layer stainless-steel cladding (AISI316L with physical properties in [14]) is used. The second layer is made of Bohrium Nitride (BNi) an electrical insulator with physical properties from [15]. To simulate the heat generation material (Incone-l600), a very thin layer assuming steel properties is located inside the BNi-layer. At the pin center, an inner copper rod is installed that is electrically insulated from the Inconel600 layer by Bohrium Nitride.

4 STUDIED CASE

To understand the origin of uncertainties in our numerical results, steady state forced convection case ADP07ss1 is considered in a detailed analysis. This case has the highest percentage error compared to other cases, see Fig. 2. Table 2 gives integral parameters of this test case. The previously validated model described above is employed for case ADP07ss1 without any modification. Selected results demonstrating velocity temperature fields and streamlines are presented and discussed below. The secondary flow velocity, i.e. lateral flow, and axial velocity contours at the measurement section A are shown in Fig. 6a and 6b, respectively. A strong mixing occurs due to the wire-wraps. This becomes apparent from the magnitude of resulting lateral and axial velocity. Note, that the maximum amplitude of lateral velocity is about 26% of the average axial velocity.

In Fig. 7, TCs far from actively heated pins or located in regions near boundaries are hardly affected by the heating result in the highest error. These could be influenced by possible heat losses to the environment in the preheated and heated section of the bundle. Therefore, excluding these TCs in the uncertainty quantification decreases the average error. For instance, TCs measuring low temperature result in a very high percentage error, e.g. TC 26 in Fig. 7 results in 605 % relative error. Excluding just TC 26 from the evaluation reduces the average error by 9%. Additionally, when the data at measurement section A, i.e. near the inlet exhibiting low temperature TC readings, is not considered in the comparison, a lower percentage error can be found. Table 3 shows the average error for all KIT benchmark results compared to the maximum and minimum values of other participants. Note that data near the inlet was excluded, i.e. following the procedure in [3]. The results in Table 3 show the remarkable observation: the average error for the natural convection cases is lower than that for forced convection cases. We assume that this is due to buoyancy forcing the flow to rise, consequently supressing part of the lateral mixing which is poorly modelled. Remember that the CFD model employs the isotropic turbulence assumption which does not properly account for swirl effect due to the wire wrap.

Considering the maximum temperature difference $|T_{CFD}-T_{exp}|$, the TC67 shows the highest discrepancy, i.e., 24.7 °C when using the first-order advection scheme for temperature, compared to 36.8 °C when using the second-order scheme (Table 1). The 24.7 °C difference results in a local error of approximately 25.7%. To understand the reason behind such ahigh local error, a closer examination of the local temperature and flow fields is necessary. The temperature contours in measurement section C are shown in Fig. 8a, which also indicates the position of cutting plane AA. The temperature contours along the plane passing through the line connecting the thermocouples (TCs) located in Pin 3 (cutting plane AA) are presented in Fig. 8b. The streamlines originating from the plane cutting through subchannel S3 at measurement plane A, along with a line in plane A, are shown in Fig. 9. The flow field is governed by the wire-wrap–induced flow pattern. The temperature in channel S3 is strongly influenced by the amount of cold flow entering S3 and by heat convection from the hot region into S3.

Considering the temperature values shown in Fig. 7, the temperature increases nearly linearly from TC55 to TC58, followed by a slight decrease at TC59 and an approximately constant temperature between TC59 and TC61. TC55 lies in measurement plane A, whereas TC61 is located in measurement plane B. The distance between planes A and B represents one axial pitch period. The temperature trend from TC62 to TC67 is similar to that in the previous axial pitch, showing intervals of nearly constant temperature and a more pronounced decrease after TC64.

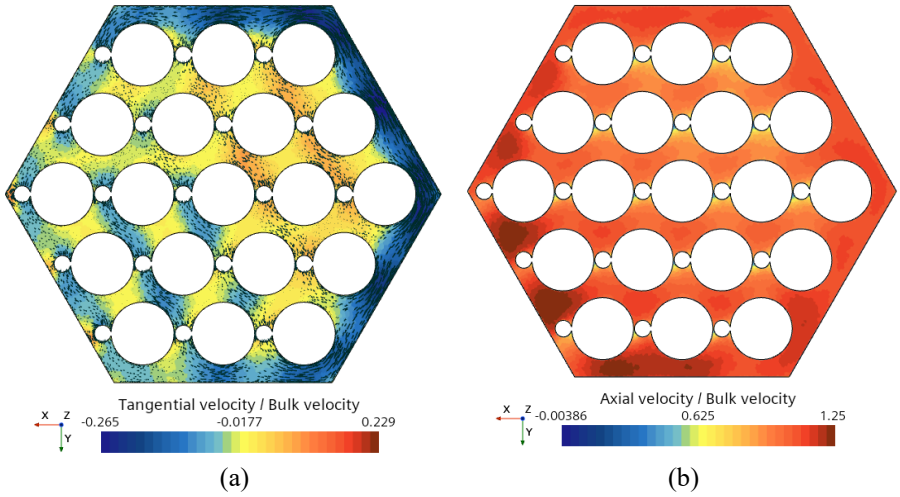

FIG. 6. Velocity contours at section A, steady state1 forced convection case ADP07SS1.

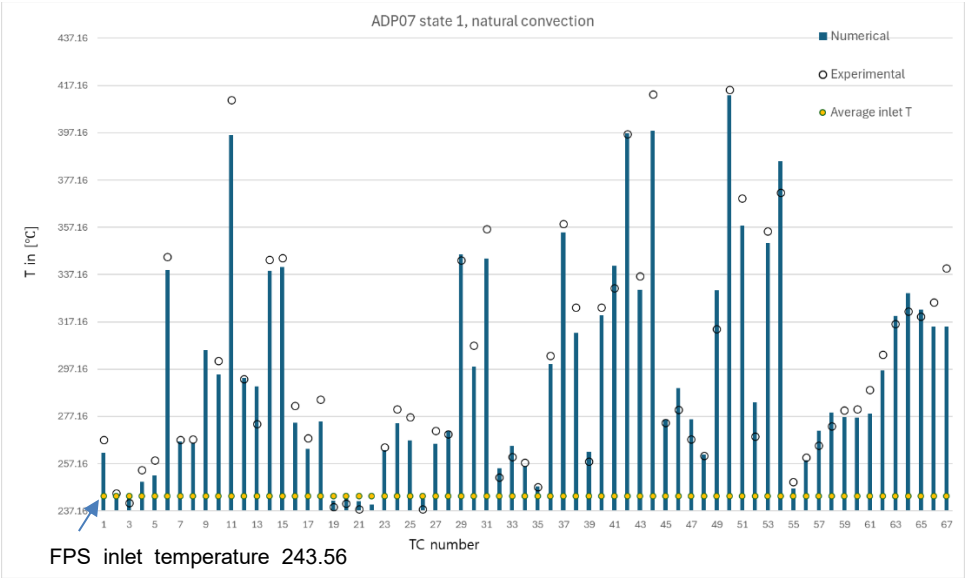

FIG. 7. Forced convection results, mesh II with long heater, steady state1 forced convection case ADP07ss1.

TABLE 3. AVERAGE ERROR FOR ALL KIT BENCHMARK RESULTS COMPARED TO THE MAXIMUM AND MINIMUM VALUES OF OTHER PARTICIPANTS, DATA FROM [16].

	Average Error (%)					
	ADP10ss1	ADP10ss2	ADP06SS1	ADP06ss2	ADP07ss1	ADP07ss2
Minimum	2.3	1.8	6.4	4.1	15.3	8.3
KIT results	4.2	2.7	9.2	7.7	17.0	9.1
Maximum	5.5	6.3	12.0	15.6	33.6	40.1

When comparing the numerically obtained temperature trend with the experimental results, Fig. 7 shows a lower temperature slope between TC55 and TC58 than that predicted numerically. This indicates that the

numerical model predicts locally weaker mixing in the S3 channel with the cold stream entering S3 compared to the experiment.

For TC59 to TC61, the experimental measurements indicate lower mixing in this region, with the temperature remaining constant between TC59 and TC60. In contrast, the numerical results show that the temperature remains constant over a longer axial distance, from TC59 to TC61. These differences are mainly attributed to the isentropic turbulence assumption. In reality, a different pattern is expected. Deficiencies in the turbulence model may lead to uncertainties in the amplitude and phase of the circulation around the rods and, consequently, in the mixing of the flow in subchannel S3. Therefore, the evaluation of numerical results should always be carried out carefully, with particular attention to possible deviations arising from model assumptions. In the studied case, a deviation of 25.7% was obtained for the asymmetrically heated case, whereas a much lower error was observed for the symmetrically heated case.

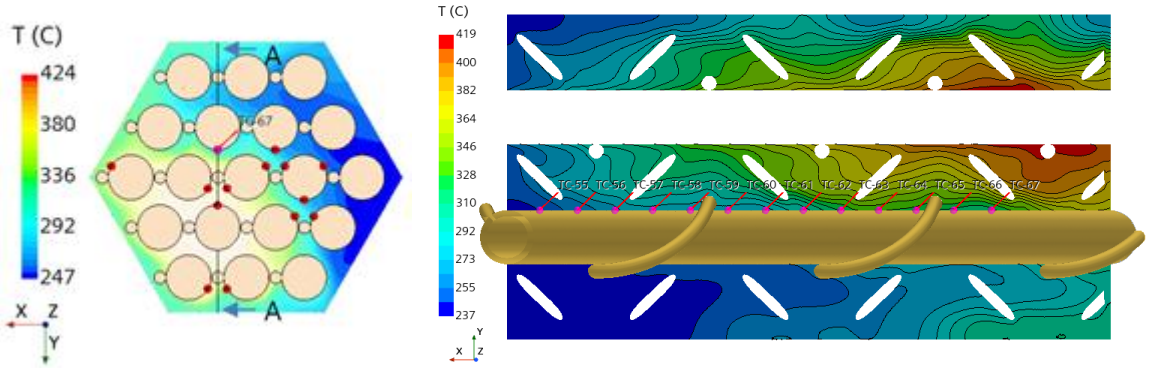

(a) (b)

FIG. 8. (a) Temperature contours and wall-TC positions at section C and (b) at cutting plane AA, steady state1 forced convection case ADP07ss1.

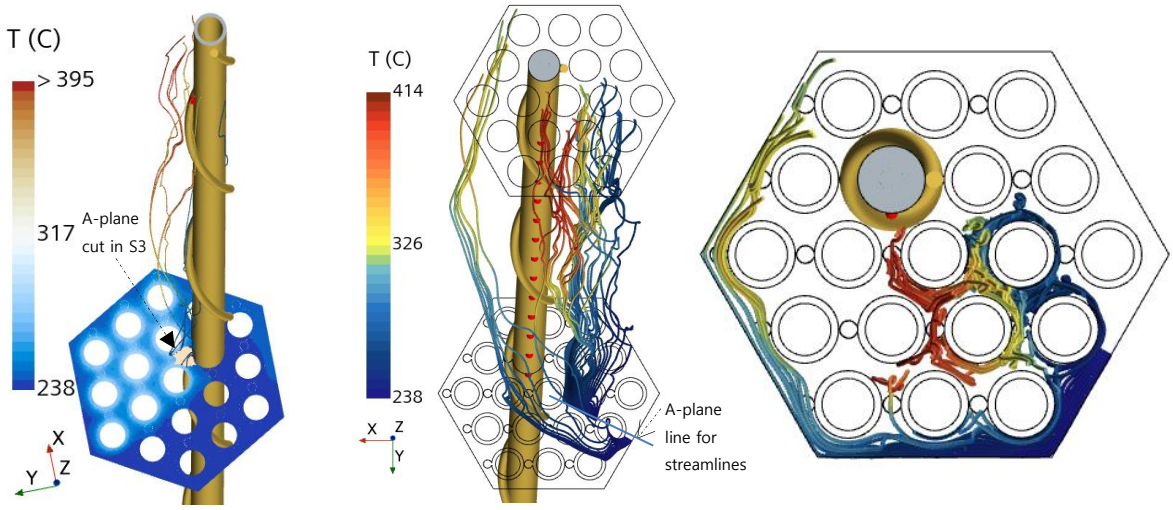

(a) (b) (c)

FIG. 9. Streamline between sections A - C started: (a) channel S3 in plane A (b) a line in plane A and (c) top view of (b), steady state1 forced convection case ADP07ss1.

The sensitivity of temperature measurements to possible TC position changes due to deformation and installation tolerances is not considered in the benchmark because of the complexity of the required model and computations. Small displacements of TC positions in a near-uniform or non-uniform temperature field can result in low or high sensitivity of the measured temperature to TC movement. Accordingly, a sensitivity study comparing the effects of small TC displacements is presented here. For this comparison, the TCs placed axially in Pin 3 (TC55–TC67) are considered. The effects of a small displacement of ±1 mm in the axial flow direction

and ±5° in the lateral TC location are examined. Fig. 10 shows a comparison between the experimentally measured temperatures and the numerically obtained results for the defined displacements. As shown in Fig. 8b, TCs located in the vicinity of high temperature gradients, such as TC61, TC64, and TC67, are more sensitive to TC position than the others. The potential temperature differences resulting from the assumed displacements explain only a small portion of the deviation between numerical and experimental results. This confirms that the sensitivity of the results is primarily related to the mixing model applied, as discussed above.

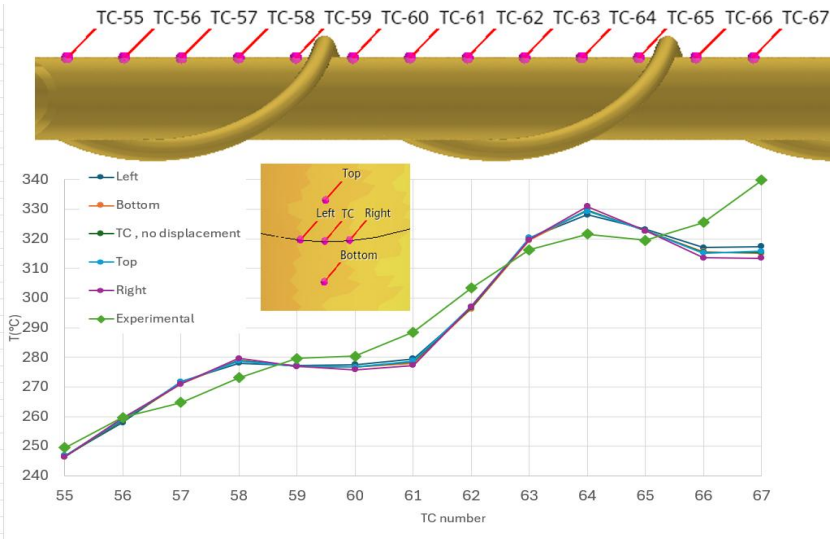

FIG. 10. Sensitivity to TC position displacement by ± 1 (Top, Bottom) mm in the axial flow direction and ± 5°(Right, left) in the lateral TC location for TC in rod 3 compared to experiment. steady state1 forced convection case ADP07ss1.

5 CONCLUSIONS

The previously verified SST turbulence model shows reliable accuracy for symmetrically heated cases and consequently it is used for blind simulation. The results of the applied model are compared to those of other benchmark participants for the blind case employing characterized by asymmetrical heating. Our results received rank 5 out of 14 compared candidates. However, it shows lower accuracy compared to the previous symmetrically heated case. Yet, TCs laying in actively heated regions show an error range comparable to that observed in the symmetrically heated cases. Thermocouples to whom we pay little attention that are mounted on pins which are not actively heated or at locations far from the actively heated region noticeable contribute to rise the average error. In the previous case of symmetrical heating, the CFD provided good results thus capturing the features of the flow and temperature fields although it has its own model uncertainties.

The current sensitivity analysis investigating TC location shows that the main reason for degraded accuracy in the asymmetrically heated case is due to limited accuracy of turbulence models capturing the real fluid mixing between the individual subchannels. This leads to elevated uncertainty in the temperature fields, when adjacent subchannels exhibit high differential temperatures. This is the case for TCs mounted on pin3 where the calculated temperature values strongly dependent on the mixing of the hot and cold region surrounding the pin. Fine tuning of mixing parameters for an individual calculation is not recommended. In the previous case of symmetrical heating, the mixing effect is considered less pronounced due to the weaker observed temperature gradients across adjacent subchannels.

For wire-wrapped fuel bundles turbulence models still show deficiencies with respect to lateral mixing. This is acceptable as this mainly influences regions where no direct heating is observed, so that uncertainty in lateral mixing dominates errors. In regions where the highest local temperatures are found, i.e. which are most relevant for safety considerations, buoyancy results in a well-defined dominant flow direction, thus reducing the overall importance of lateral mixing. We believe that state of the art CFD with RANS models is sufficient for design purposes. For large bundles typically featuring near-uniform heating the accuracy in regions of interest results are expected to become even more accurate. In general, the CFD results meet experts' expectations, showing high accuracy with respect to integral heating and some uncertainty regarding lateral heat transport. In the design

process, critical conditions can be identified through CFD, and design optimization should aim to minimize CFD-related uncertainty in regions where temperature limits may be exceeded.

The present sensitivity study focused on the effects of displacement, deformation, or inaccurate measurement positions. It partially explains the deviations between numerical and experimental results for TCs located in regions with high temperature gradients.

ACKNOWLEDGMENTS

This work has been supported by the Framatome Professional School at KIT. The data and information presented in the paper are part of an ongoing IAEA coordinated research project on "Benchmark of Transition from Forced to Natural Circulation Experiment with Heavy Liquid Metal Loop – CRP-I31038. The work presented is original but some or all of the information may need to be included in a book publication at a later date as part of the output of the International Atomic Energy Agency coordinated research project on "Benchmark of Transition from Forced to Natural Circulation Experiment with Heavy Liquid Metal Loop – CRP-I31038.

REFERENCES

[1] Di Piazza, H. Hassan, P. Lorusso, D. Martelli, “Benchmark specifications for nacie-up facility: non-uniform power distribution tests”, Ref. NA-I-R-542, Issued: 28/02/2023 ENEA, Italy

[2] Di Piazza, et.al. “The IAEA Benchmark on Transition from Forced to Natural Circulation with NACIE Heavy Liquid Metal Loop”, NURETH-21, paper ID 1770, Busan, Korea, 2025

[3] Mathur, A. et.al. “CFD Benchmark for Non-uniform Heating Experiments in NACIE Rod Bundle”, NURETH-21, paper ID 1803, Busan, Korea, 2025.

[4] Batta, A. Class A., “CFD Validation of forced and natural convection for the open phase of IAEA Benchmark CRP - I31038”, SCOPE (Saudi International Conference On Nuclear Power Engineering) 13–15 Nov 2023 King Fahd Conference Center, KFUPM, Dhahran, KSA

[5] Batta, A. Class A., “IAEA Benchmark CRP - I31038: Open Phase liquid-metal CFD results for fuel pin simulator”, paper no 222, NUTHOS-14, Vancouver, BC, Canada, 2024

[6] Batta, A. Class A., G. “CFD Validation on Liquid Metal Flow in 19 Wire Wrapped Bundle Flow Investigated in The IAEA Coordinated Research Project CRP-I31038 Using NACIE Experimental Data”, NURETH-21, paper ID 1811, Busan, Korea, 2025.

[7] Roelofs, F. et al., “Towards validated prediction with RANS CFD of flow and heat transport in a wire-wrap fuel assembly,” Nuclear Engineering and Design 353, 110273 (2019).

[8] K. Sergeenko, “Adaption of the turbulence model to the heat transfer in a rod bundle,” *Nuclear Engineering and Design* 415, 112664 (2023).

[9] Batta, A. Class, “CFD validation for partially blocked wire-wrapped liquid-metal cooled 19-pin hexagonal rod bundle carried out at KIT-KALLA”, Proc. of the 19th International Topical Meeting on Nuclear Reactor Thermal Hydraulics (NURETH-19) Log nr.: 36240 Brussels, Belgium, March 6 - 11, 2022

[10] Batta, A. et al., “Validation for CFD thermalhydraulic simulation for liquid metal cooled blocked 19-pin hexagonal wire wrapped rod bundle experiment carried out at KIT-KALLA”, AMNT 50, 2019

[11] Batta, A.: Class, A. Thermalhydraulic CFD validation for liquid metal cooled 19-pin hexagonal wire wrapped rod bundle, paper 28473, NURETH-18.

[12] Batta, A.: et al., “Numerical analysis of a LBE-cooled blocked 19-pin hexagonal wire wrapped rod bundle experiment carried out at KIT-*KALLA* within EC-FP7 project MAXSIMA” Paper ID 20532, NURETH-17

[13] N. E. Agency, “Handbook on Lead-bismuth Eutectic Alloy and Lead Properties, Materials Compatibility, Thermal-hydraulics and Technologies,” Nucl. Sci., pp. 647–730, 2015.

[14] Kim, C.S. “Thermophysical properties of stainless steels”, ANL-75-55, 1975.

[15] Thermocoax, private communication

[16] Mathur, A. “IAEA CRP Benchmark of Transition from Forced to Natural Circulation Experiment with Heavy Liquid Metal Loop, WP2 Summary” 4th RCM Vienna, 21-25 October2025